doi:10.1111/j.1365-2591.2007.01370.x

Characterization of hydration products of mineral trioxide aggregate

J. Camilleri
Department of Building and Civil Engineering, Faculty of Architecture and Civil Engineering, University of Malta, Malta

Abstract

Camilleri J. Characterization of hydration products of mineral trioxide aggregate. *International Endodontic Journal*, **41**, 408–417, 2008.

Objective To characterize the hydration products of white mineral trioxide aggregate (MTA).

Methodology Mineral trioxide aggregate, white Portland cement and bismuth oxide were evaluated using X-ray diffraction (XRD) analysis and Rietveld XRD. The cements were tested un-hydrated and after hydration and curing for 30 days at 37 °C. Analysis of hydrated cement leachate was performed weekly for five consecutive weeks from mixing using inductively coupled plasma atomic emission spectroscopy after which the cements were viewed under the scanning electron microscope to evaluate the cement microstructure. Quantitative energy dispersive analysis with X-ray was performed and atomic ratios were plotted.

Results Both Portland cement and MTA produced calcium silicate hydrate (C-S-H) and calcium hydroxide (CH) on hydration. The tricalcium aluminate levels were low for MTA which resulted in reduced production of ettringite and monosulphate. On hydration the bismuth level in the hydrated MTA decreased; bismuth oxide replaced the silica in the C-S-H and was leached out once the C-S-H decomposed with time. Both MTA and Portland cement released a high amount of calcium ions which decreased in amount over the 5-week period.

Conclusions The hydration mechanism of MTA is different to that of Portland cement. In MTA the bismuth oxide is bound to the C-S-H and is leached out from the cement with time as the C-S-H decomposes. MTA produces a high proportion of calcium ions from CH a by-product of hydration and also by decomposition of C-S-H. The release of calcium ions reduces with time.

Keywords: hydration, mineral trioxide aggregate, Portland cement.

Received 11 September 2007; accepted 30 October 2007

Introduction

Mineral trioxide aggregate (MTA) is composed of ASTM Type 1 Portland cement with a 4 : 1 addition of bismuth oxide added for radio-opacity (Torabinejad & White 1995). The elemental constitution of MTA is similar to that of Portland cement (Estrela *et al.* 2000, Funteas *et al.* 2003, Asgary *et al.* 2004) and both cements are composed primarily of tri- and dicalcium silicate as verified by X-ray diffraction (XRD) analysis (Camilleri *et al.* 2005a). The levels of toxic chemicals in Portland cement are low and similar to those of MTA (Duarte *et al.* 2005). So it can be postulated that MTA can be replaced by a cheaper Portland cement. MTA is deficient in alumina suggesting that the material is not prepared in a rotary kiln as is customary for the manufacture of Portland cement (Camilleri 2007). Thus, although both MTA and Portland cement have similar major constituent elements there is a variation in the other compounds present. The low levels of alumina affect the production of ettringite and monosulphate usually formed on hydration of Portland cement (Camilleri 2007).

The first publication on the chemical and physical properties of MTA (Torabinejad *et al.* 1995) did not report the presence of bismuth oxide in the material.

Correspondence: Dr Josette Camilleri, Department of Building and Civil Engineering, Faculty of Architecture and Civil Engineering, University of Malta, Malta (Tel.: 00356 2340 2870; fax: 00356 21 330190; e-mail: josette.camilleri@um.edu.mt).

The bismuth oxide seemed to have been added later to enhance the radio-opacity of MTA. Bismuth oxide affected the hydration mechanism of the MTA; it formed part of the structure of the calcium silicate hydrate (C-S-H) and also affected the precipitation of calcium hydroxide (CH) in the hydrated paste (Camilleri 2007). The levels of bismuth and calcium leached out from MTA are as yet unknown. The level of bismuth that is actually bound to the C-S-H gel structure has also not been investigated.

The objective of this study was to characterize the hydration products of white MTA and compare them to those of white Portland cement.

Materials and methods

White MTA (Tulsa Dental Products, Tulsa, OK, USA; Batch number: 756464/02) and white Portland cement (Castle White Portland cement; BS EN 197-1: 2000, Type CEM 1; strength class 52,5N) were used in this study.

Chemical analysis of the materials

Chemical analysis was performed on both hydrated and un-hydrated MTA and Portland cement and bismuth oxide (Fischer Scientific, Leicester, UK). MTA was mixed with the liquid provided in capsules to produce a liquid-to-MTA ratio of 0.5. One gram of white Portland cement was mixed with 0.5 g distilled water, to give a water/cement (w/c) ratio of 0.5. The two pastes were cured at 37 °C in water for 30 days after which they were washed with isopropyl alcohol to desiccate them prior to performing the analysis.

X-ray diffraction analysis

For XRD analysis 20% rutile (Titanium dioxide; Sigma-Aldrich, Gillingham, UK) was added to each material to be used as internal standard. The hydrated cements were crushed to a very fine powder using a mortar and pestle. The phase analysis of both cements hydrated and un-hydrated and bismuth oxide was performed using XRD analysis. The diffractometer (Ital Structures Compact 3K5, Riva del Garda, Italy) used Cu Kα radiation at 30 mA and 40 kV. Samples were presented in powder form and were compacted on a sample holder. The crystalline structure of the test cement was determined by passing a beam of X-rays of known wavelength into the specimen whilst rotating it through an angle θ. The intensity of X-rays from the sample was measured by a detector. The detector was rotated between 10° and 60° at 0.02° 2θ per 0.5 s and also between 45° and 55° at 0.005° 2θ per 0.1 s. Phase identification was accomplished by use of search-match software utilizing the International Centre for Diffraction Data (ICDD) database (International Centre for Diffraction Data, Newtown Square, PA, USA).

Rietveld X-ray diffraction analysis

Materials under study were hydrated and un-hydrated cements and bismuth oxide. Twenty per cent corundum (Al_2O_3) relative to the weight of cement was blended with the cement powder to serve as an internal standard. This material was chosen because it does not react with water and has no influence on the hydration reaction. Rietveld analysis was performed on ground sample. X-ray diffraction patterns were first obtained with sufficient resolution for Rietveld analysis. The detector was rotated at 0.017° 2θ per 20 s.

Chemical analyses of cement leachate

The chemical analysis of the cement products released into solution was performed using inductively coupled plasma atomic emission spectroscopy (ICP-AES; Varian Medical Systems, Palo Alto, CA, USA). MTA and Portland cement were mixed as described in the previous experiment, and cured for 3 days at 37 °C and 100% humidity. They were then weighed and placed in closed plastic sterile containers (Labplex, Birmingham, UK) to which was added 100 mL of deionized water. Containers filled with deionized water were used as controls. The samples were allowed to cure at 37 °C for 5 weeks. The water within the bottles was changed on a weekly basis with the leachate water being collected for analysis. The leachate was analysed for aluminium, bismuth, calcium, iron, potassium, magnesium, phosphorus, sodium and silicon. The amount of leachate was calculated in μg/g by using the following formula:

$$\text{Amount of leachate per weight of cement} = \frac{\text{amount of leachate per litre} \times 100}{\text{weight of cement pellet}}$$

Scanning electron microscopy of set leached cements

After completing the leaching experiments for five consecutive weeks the cements were immersed in acetone for 30 days to remove any remaining water, and then dried in a vacuum desiccator for 8 h. The dried paste pieces were set in epoxy resin using vacuum

impregnation. The hardened resin block was sawn (Labcut 1010; Agar scientific, Stansted, UK) and ground under copious water irrigation using progressively finer grits of abrasive paper to produce a flat surface. Fresh resin was applied to the flat surface to fill pores not filled with resin when originally embedded. Finally, the hardened surface was reground and polished. A thin conductive coating of evaporated carbon was applied to the sections prior to examination in the scanning electron microscopy (SEM; ISI SS40, ISI, Tokyo, Japan). Analysis of microstructure of the cements was performed qualitatively and quantitatively by identifying and labelling the hydration products viewed under the SEM in back scatter mode and also by examining the sections in more detail by collecting a series of 60 quantitative analyses (SAMx Numerix, Levens, France) of the hydration products and plotting the data as atomic ratios. Quantitative analysis was carried out using X-ray standards obtained from minerals for each element, with the exception of bismuth. A bismuth standard was obtained from bismuth oxide in uncured MTA. Oxygen was calculated by stoichiometry. Atomic ratios were used rather than the absolute values as the proportion of water present could not be quantified. Plots of Al/Ca versus Si/Ca were drawn.

Results

Chemical analysis of the materials

X-ray diffraction analysis

The XRD patterns between 10° and 60° 2θ of the cements and bismuth oxide are shown in Fig. 1 and the diffraction patterns for the materials between 45° and 55° 2θ are shown in Fig. 2. Both MTA and Portland cement showed the major peaks of tricalcium silicate at 32.18, 32.54° 2θ (Fig. 1a,c) and at 51.67° 2θ (Fig. 2a,c). These peaks reduced in intensity in the hydrated phases (Figs 1b,d and 2b,d). In addition both hydrated materials had very strong peaks for CH at 18° 2θ (Fig. 1b,d) and 54.36° 2θ (Fig. 2b,d). The bismuth oxide had two very strong peaks at 27.30 and 46.30° 2θ (Figs 1e and 2e). The bismuth oxide peaks were present in the MTA (Figs 1a,b and 2a,b) but not in the Portland cement samples (Figs 1c,d and 2c,d). In the hydrated MTA the bismuth oxide peak intensities at 27.30° 2θ (Fig. 1b) and at 46.30° 2θ (Fig. 2b) were lower than in the un-hydrated paste (Figs 1a and 2a). The bismuth oxide peak at 27.30° 2θ coincided with the rutile peak. Further peak superimposition occurred at 54° 2θ with major peaks for CH being superimposed on rutile and bismuth oxide.

Rietveld x-ray diffraction analysis

The quantitative x-ray analysis performed on the un-hydrated cements using the Rietveld diffractometer are shown in Table 1. The MTA had a lower level of tricalcium silicate and a higher level of dicalcium silicate when compared to white Portland cement. There was no tricalcium aluminate present in the MTA. Tetracalcium alumino-ferrite was absent in both MTA and Portland cement. Calcium sulphate levels were either low or absent in MTA. MTA had a bismuth oxide level of 21.6%. In the hydrated samples there was a strong reduction in tricalcium silicate levels with an increase in amorphous material level. CH and ettringite were produced by both cements. The ettringite levels in MTA were lower than that of Portland cement. The amount of bismuth present in MTA was lower in the hydrated cement. The Rietveld analysis however could not make out where the bismuth was located.

Chemical analyses of cement leachate

The amount of elements leached out from white MTA is shown in Fig. 3a and that leached out of white Portland cement in Fig. 3b. Both cements showed the same trends whereby calcium, potassium and sodium levels decreased over the 5-week period, whilst the magnesium and silicon increased. The levels of bismuth leached out of the MTA increased over the 5-week period. A comparison of calcium and bismuth ions leached out of both materials is shown in Table 2.

Scanning electron microscopy of set cements

The surface of the MTA pellet was more affected than that of the Portland cement. Macroscopically the surface of the MTA pellet showed an altered surface. There was a change in colour and porosity of the material. When viewed under the SEM the MTA paste showed indications of leaching throughout most of the pellet. The leaching was arbitrarily divided into various zones namely Zone A, B, C, and D (Fig. 4). Zone A was a very thin layer approximately 100 μm wide. This area was strongly leached with no CH present and the C-S-H was strongly decalcified (Figs 4 and 5). Zone B was approximately 500 μm thick. This zone was also strongly leached with loss of CH and decalcification of C-S-H gel, but the leaching was less severe. Zone B contained a distinct layer called Zone C (Fig. 4). This

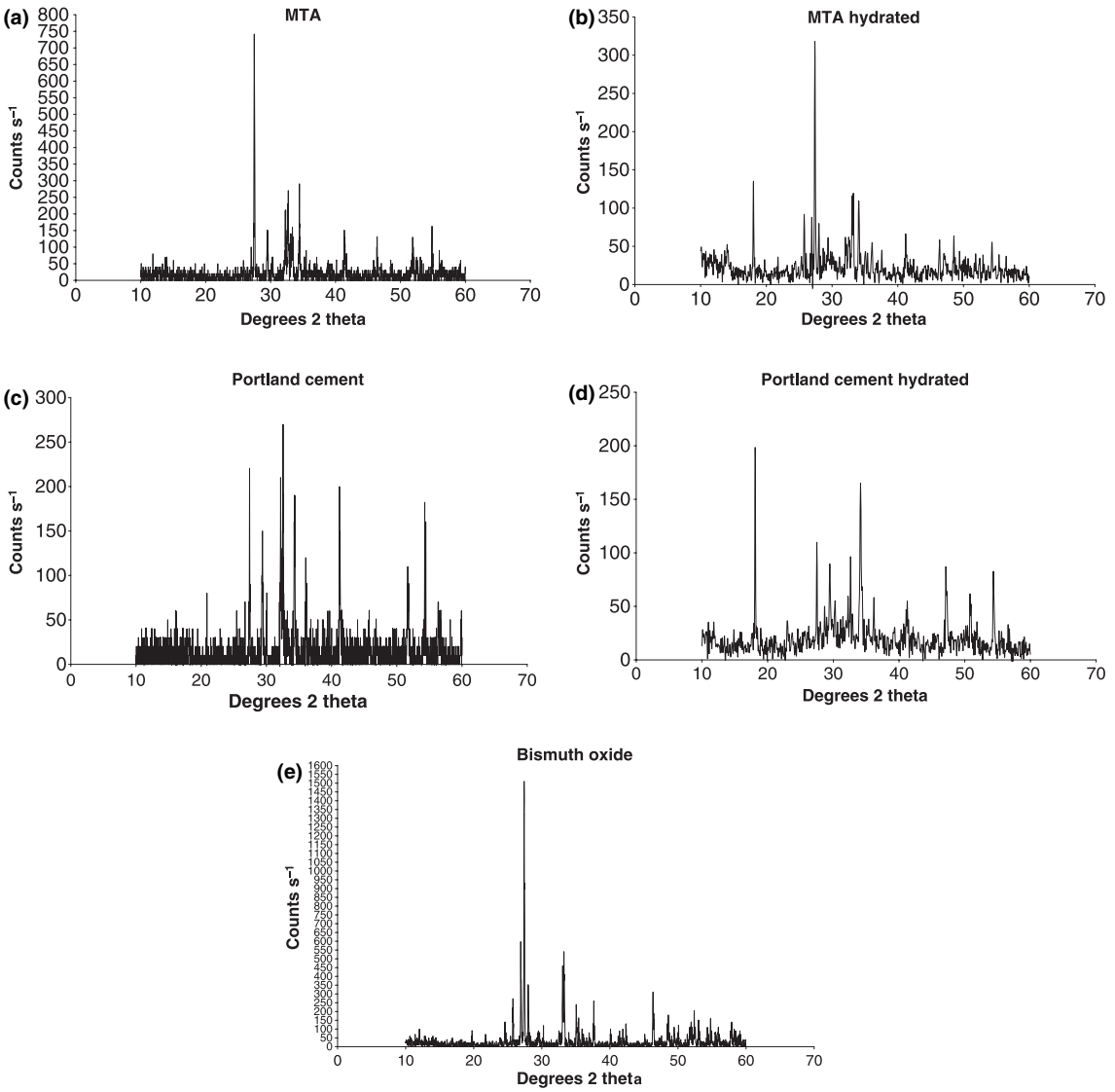

Figure 1 X-ray diffraction patterns of (a) white mineral trioxide aggregate (MTA), (b) white MTA hydrated after 30 days of curing (c) white Portland cement, (d) white Portland cement hydrated after 30 days of curing and (e) bismuth oxide. The detector was rotated between 10° and 60° at 0.02°θ per 0.5 s.

region was lens shaped and exhibited very severe leaching similar to that found in Zone A. The rest of the pellet beneath Zone B was labelled as Zone D. Although in this region there was some evidence of leaching, however, this phenomenon was less marked (Fig. 6). The white Portland cement showed extensive leaching in a thin layer from the surface to a depth of approximately 200 μm (Fig. 7). The leached surface layer consisted of a porous structure composed of occasional un-hydrated cement grains in a matrix of partially-decalcified C-S-H. Very little CH was present in this zone (Fig. 8). Beneath the leached surface layer, the paste appeared essentially normal for a cement paste composed of white cement with a water-cement ratio of 0.5. The main hydration products were C-S-H and CH. Numerous residual partly-hydrated cement grains and appreciable capillary porosity were present (Fig. 7). The plot of Si/Ca v Al/Ca for the MTA (Fig. 9) showed all the points falling close to a straight line. This indicated the presence of a mixture of C-S-H and CH (up to Si/Ca = 0.5) and decalcified C-S-H (Si/Ca > 0.5). Most of the aluminium was present

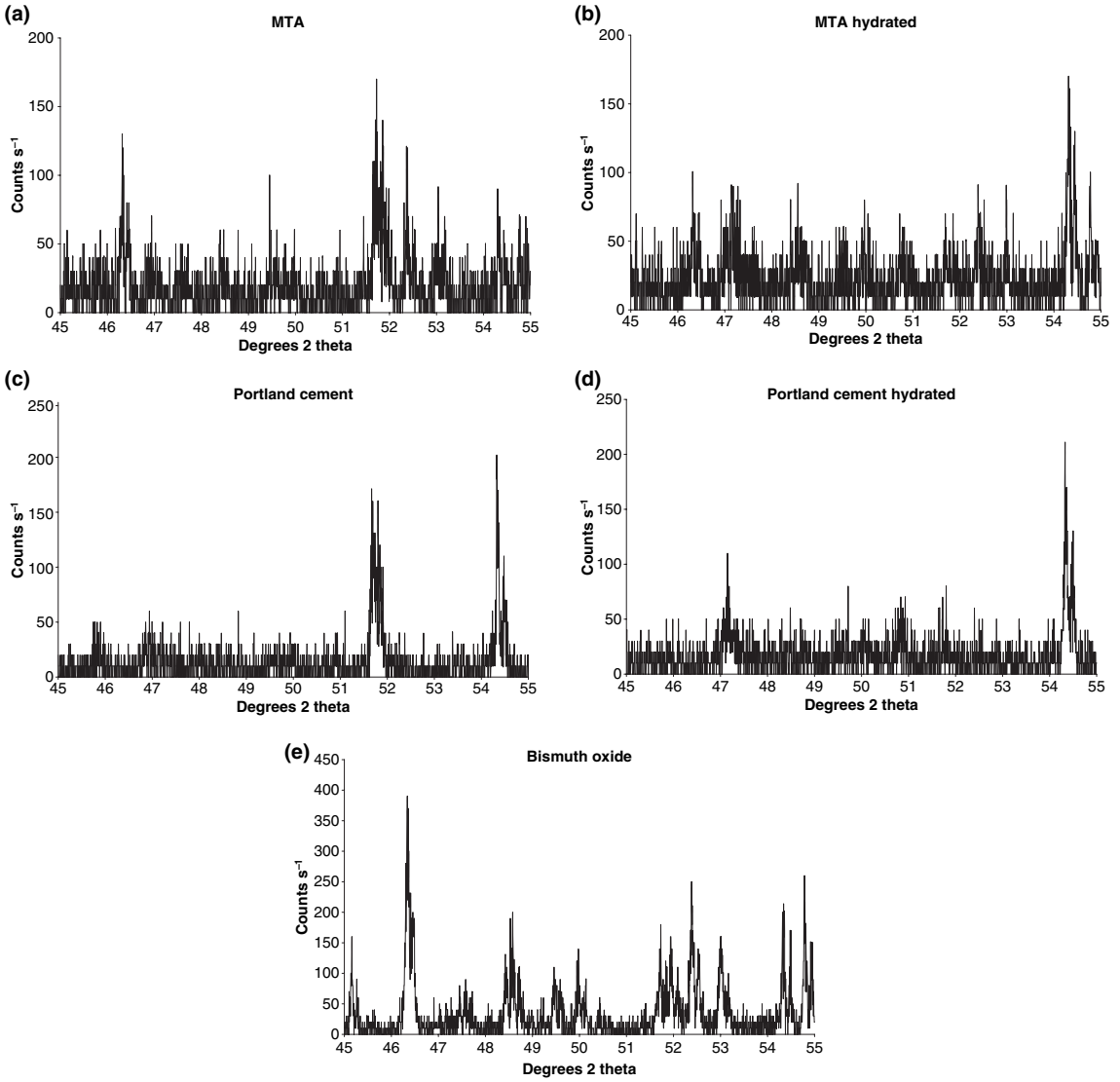

Figure 2 X-ray diffraction patterns of (a) white mineral trioxide aggregate (MTA), (b) white MTA hydrated after 30 days of curing (c) white Portland cement, (d) white Portland cement hydrated after 30 days of curing and (e) bismuth oxide. The detector was rotated between 45° and 55° at 0.005°θ per 0.1 s.

within the C-S-H, as the Al/Si ratio remained constant. The plot for Bi/Si for MTA is shown in Fig. 10. There was a linear relationship between the bismuth and silicon as shown by the straight line AB indicating a direct relationship between the silicon and the bismuth ions. The plot for Si/Ca v Al/Ca for the Portland cement (Fig. 11) showed a cluster (A) corresponding to normal *in-situ* hydration product C-S-H. Higher ratios of Si/Ca indicate decalcification due to leaching. Ratios of Si/Ca below 0.5 represent mixtures of C-S-H and CH. In this case the monosulphate phase is present unlike in the MTA where the monosulphate phase was scarce.

Discussion

Compound composition identification can be performed by XRD analysis. Other techniques used for chemical analysis such as Energy Dispersive Analysis with X-ray only give information about the elements present within the material without showing the compound composition. XRD identifies crystalline phases contained in unknown samples; amorphous structures cannot be characterized using this technique. XRD is useful in performing chemical analyses of un-hydrated cement as Portland cement is crystalline (Camilleri

Table 1 Cement phases detected by Rietveld X-ray diffraction analysis

	Weight fractions			
	Un-hydrated cement		Hydrated cement	
Phases	OPC	MTA	OPC	MTA
Tri-calcium silicate	74.7	53.1	8.2	10.6
Di-calcium silicate	7.4	22.5	0	14.9
Tetra-calcium alumino ferrite	0	0	0	0
Tri-calcium aluminate	3.6	0	0	0
Gypsum	1.1	0	0	0
Hemi-hydrate	1.1	0.7	0	0
Anhydrite	2.7	1.5	0	0
Calcium hydroxide	2.1	1.0	15.7	14.4
Calcium carbonate	5.0	1.4	3.2	0
Bismuth oxide	0	21.6	0	8.4
Ettringite	0	0	7.5	2.1
Calcium silicate hydrate	0	0	62.2	49.5

OPC, ordinary Portland cement; MTA, mineral trioxide aggregate.

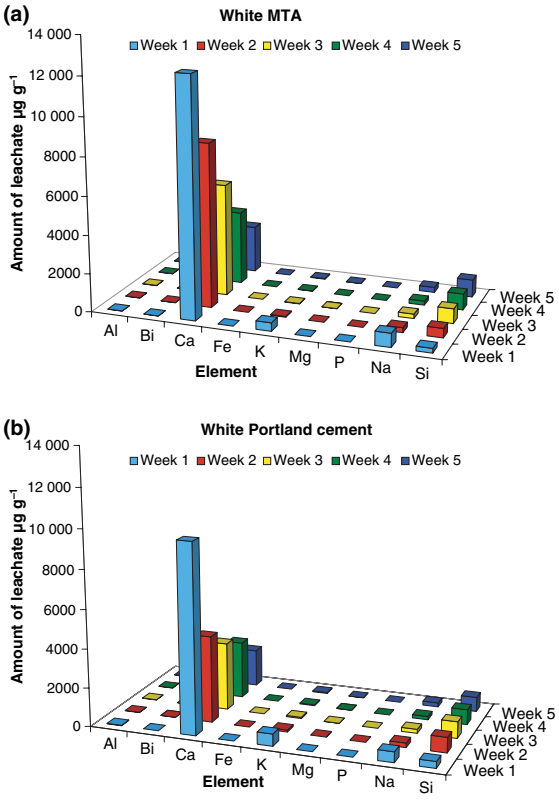

Figure 3 Ion release by (a) white mineral trioxide aggregate, (b) white Portland cement over a period of 5 weeks.

et al. 2005a). Diffraction patterns of cementitious materials provide phase, chemical, and crystal structure information data that will be needed to aid understanding of cement performance. Portland cement has unique diffraction patterns for each phase and each pattern is produced independently of others. In addition in a mixture the intensity of each phase is proportional to the phase concentration. With the use of internal standards such as rutile and corundum amorphous phases can be identified and the phase concentration quantified. The main disadvantage with the use of XRD to analyse Portland cement is the substantial peak overlap caused by the large number of phases present in the material. This problem is addressed by using the Rietveld method (Rietveld 1969) which allows standardization of powder diffraction analysis through use of calculated reference diffraction patterns based upon crystal structure models. The principle of Rietveld analysis is to iteratively compare the experimental pattern with a pattern simulated based on the presumed amounts, crystal parameters, and equipment parameters of a mixture of

Table 2 Calcium and bismuth ion release from mineral trioxide aggregate (MTA) and Portland cement over a period of 5 weeks

	MTA		Portland cement	
	Bismuth µg/g	Calcium µg/g	Bismuth µg/g	Calcium µg/g
Week 1	3.62	12368.00	0.68	9692.83
Week 2	7.23	8534.64	<0.68	4436.86
Week 3	13.74	5858.53	<0.68	3481.23
Week 4	10.13	3833.36	<0.68	2935.15
Week 5	16.64	2459.13	<0.68	1911.26

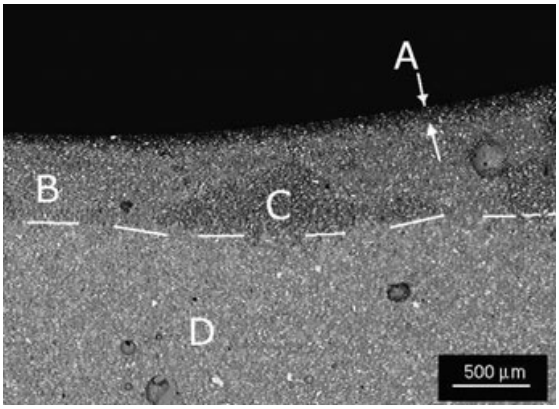

Figure 4 Leached mineral trioxide aggregate paste pellet, view of surface region, showing: a highly porous surface layer (Zone A) approximately 100 µm wide; a denser zone comprising the bulk of the pellet (D); a zone of intermediate porosity (B); a 'lens' of leached paste (C) within Zone B.

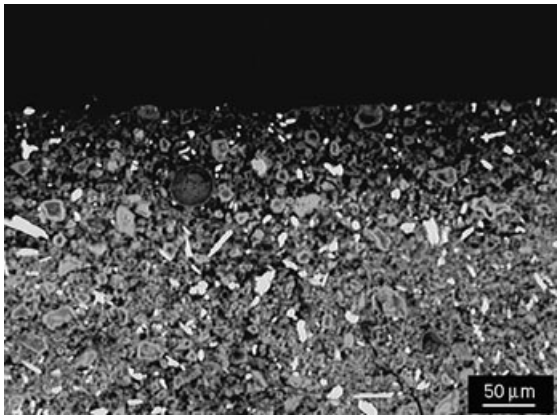

Figure 5 Leached mineral trioxide aggregate paste pellet, showing Zones A and B. Most of the undifferentiated hydration product has been leached from Zone A and the remaining paste consists largely of tenuously-bonded *in-situ* hydration product formed of partly-decalcified calcium silicate hydrate. A similar process has occurred in Zone B but to a lesser extent. The very bright features are bismuth oxide particles.

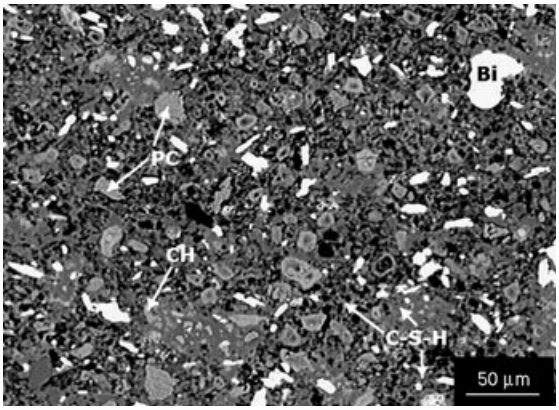

Figure 6 Leached mineral trioxide aggregate paste pellet, detail of Zone D 1 mm from surface showing low levels of calcium hydroxide (CH), bright particles of bismuth oxide (Bi), residual un-hydrated cement grains (PC) and calcium silicate hydrate (C-S-H).

known phases. All these parameters may be adjusted between iterations to minimize the difference between experimental and simulated patterns by least squares fitting. Simultaneous refinement of XRD patterns of multiple phases allows quantitative analysis (Gilfrich *et al.* 1998). Whilst XRD is a powerful technique for the study of crystalline materials, the technique of Rietveld refinement enables the amounts of different phases in anhydrous cementitious materials to be determined to a good degree of precision (Scrivener *et al.*

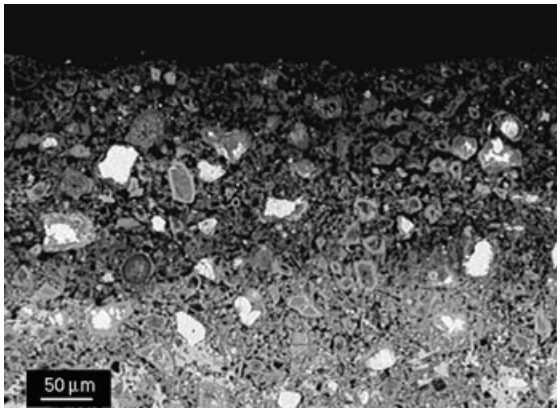

Figure 7 Leached white cement pellet, showing porous outer zone approximately 200 µm wide and a denser inner zone. Bright features are residual un-hydrated cement particles.

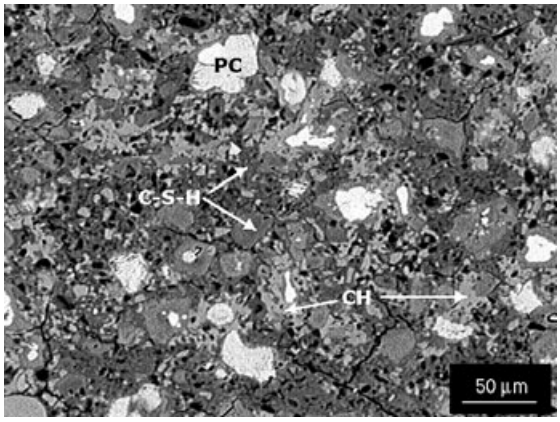

Figure 8 Leached white cement paste pellet, view of paste at centre of pellet showing bright white particles of residual un-hydrated cement grains (PC), darker grey matrix material which is calcium silicate hydrate (C-S-H) and brighter matrix material which is calcium hydroxide (CH).

2004). Inductively coupled plasma atomic emission spectroscopy uses an aqueous solution, a portion of which is aspirated in the form of fog into an argon plasma torch at about 10 000 °K, where most contained elements are excited and emit light that is characteristic of the contained elements. This technique allows simultaneous multi-element analysis both quantitatively and qualitatively with detection limits between parts per billion to parts per million. Atomic line spectra are produced for specific element and the intensities of the bands are monitored by a photomultiplier tube. Advantages of ICP include moderate costs, fairly rapid analysis time and high sensitivity (Mauras

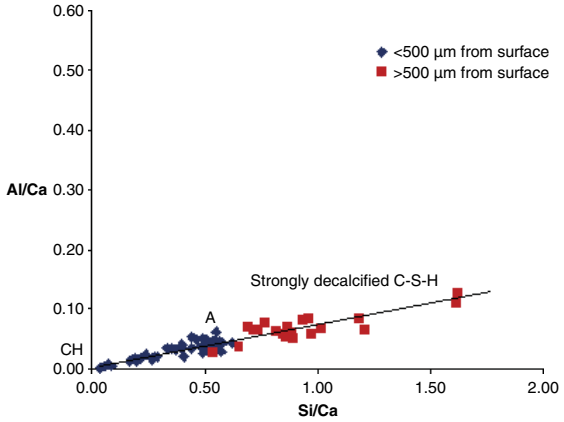

Figure 9 X-ray microanalysis data of mineral trioxide aggregate showing atomic ratios for Si/Ca v Al/Ca. Data points where Si/Ca > 0.5 indicate decalcified C-S-H (mainly red). The cluster at A indicates C-S-H of normal Si/Ca ratio and points between A and the origin are mixtures of C-S-H and CH.

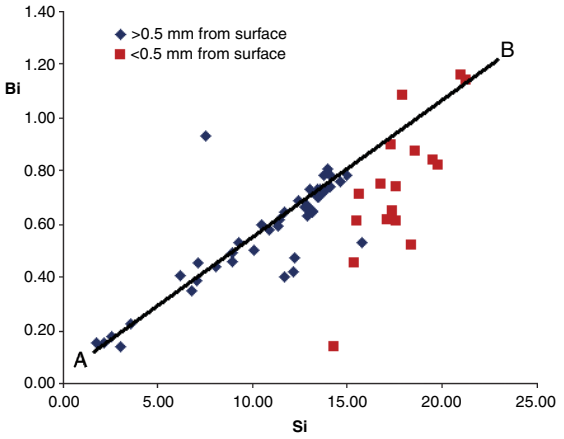

Figure 10 X-ray microanalysis date of mineral trioxide aggregate (MTA) showing atomic ratios of Si v Bi at different locations on the MTA pellet. The majority of the points falling below the line correspond to analysis locations within 0.5 mm of the pellet surface.

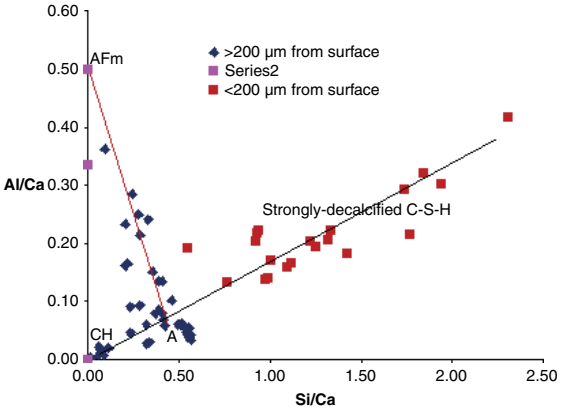

Figure 11 X-ray microanalysis data of white Portland cement showing atomic ratios for Si/Ca v Al/Ca. At 'A' is a tight cluster of data points corresponding to *in-situ* C-S-H hydration product; the Si/Ca ratio of this cluster (approx. 0.05) suggests that any leaching has been minimal. The black line from the origin to Cluster A represents data points corresponding to a mixture of C-S-H and CH; to the right of Cluster A, the black line represents partly-decalcified C-S-H, from which lime was lost due to leaching. Almost all the decalcified material was within 200 µm of the pellet surface (red data points).

& Allain 1979, Oppenheimer *et al.* 1984). Many elements can be analysed quickly and simultaneously and detection levels are very good. Most elements excited at high temperatures emit light that can be quantified very well (Montaser 1998). The main disadvantage is the presence of spectral interferences. The spectral interferences are caused when a sample contains elements or compounds that have analytical emission bands that overlap the line chosen for the analyte (Oppenheimer *et al.* 1984). Other disadvantages include the limitation of sample presentation as samples have to be able to vaporize to be tested using this technique (Montaser 1998). The results for the phase analysis using normal powder XRD were inconclusive due to peak overlap. Attempts at quantification of the phases present using an internal standard was also difficult as the rutile peak coincided with one of the main bismuth peaks. Rutile is usually used as an internal standard for testing cements (Taylor 1997). Further peak inference occurred at 54° 2θ where there was superimposition of CH, bismuth oxide and rutile. There was a reduction in the level of tricalcium silicate in the hydrated cement samples as shown by both XRD analysis and Rietveld XRD as C-S-H gel is amorphous thus does not produce any definite peaks (Taylor 1997). C-S-H was the main product of the hydration reaction as verified by Rietveld analysis. In both hydrated cements there was a high level of CH, shown by both XRD analysis results and Rietveld, which is in accordance to previous publications on the materials (Taylor 1997, Camilleri *et al.* 2005a, Camilleri 2007). This demonstrates that on hydration both MTA and Portland cement produce C-S-H gel and CH. The CH is produced from the hydration of tricalcium and dicalcium silicate. This is in contrast to what was reported previously (Dammaschke *et al.* 2005) that the CH was produced from the tricalcium aluminate

hydrogenation. The Rietveld XRD also showed a low level of tricalcium aluminate and gypsum in MTA which is in accordance with a previous study (Camilleri 2007) where the level of tricalcium aluminate was shown to be very low thus indicating that the cement is not produced in a kiln but rather in a laboratory. The levels of ettringite in the hydrated MTA were also much lower than in the Portland cement. The low levels of ettringite result form low levels of tricalcium aluminate in the MTA powder. The results of SEM analysis further confirm this as there was no monosulphate present in MTA hydrated paste. The lack of aluminium caused the reduced production of monosulphate in the hydrated paste. This is again in accordance to a previous publication (Camilleri 2007). The bismuth oxide levels were 21.6% which is in accordance to manufacturer's instructions which claim a 4 : 1 addition of bismuth oxide to MTA powder. The bismuth oxide peaks in the hydrated MTA were lower than those in the un-hydrated powder. This was shown in both XRD analysis and the Rietveld refinement demonstrating that bismuth oxide does not act as filler in MTA but rather takes an active part in the hydration mechanism of the cement. This is again in accordance to previous publications (Camilleri 2007). In the latter study it was reported that bismuth oxide formed part of the structure of C-S-H and also affected the precipitation of CH in the hydrated paste. The location of bismuth oxide in the hydrated cement could not be determined using this kind of analysis. The inductively coupled plasma atomic absorption spectroscopy results showed that the leachate had reducing levels of calcium with time. This was further confirmed with the SEM results of leached samples which showed extensive leaching of calcium for both MTA and Portland cement. More calcium was leached out from MTA than from Portland cement. This was demonstrated in both the SEM study where the leaching was more extensive in MTA than in Portland cement and also from the ICP-AES results where the calcium ion levels were higher for the MTA. The loss of calcium from the cements is through dissolution of CH and by progressive decalcification of the C-S-H. The leached calcium is simultaneously produced from the CH which, taking into consideration the hydration equilibria is dissolved before the other phases, and also from decomposition of C-S-H, which is leached out at a slower rate (Taylor 1997). The leaching also affects the ettringite and monosulphate phases of the hydrated cement. CH is dissolved first followed in sequence by monosulphate, ettringite and C-S-H (Adenot & Buil 1992). The ettringite is dissolved after the monosulphate phase as ettringite decomposes at a lower pH than the monosulphate (Gabrisova *et al.* 1991). This is in accordance with the findings of the present study where calcium leached out at fast rate, whilst the silica showed a gradual rise in levels with time due to decomposition of the C-S-H. The sodium and potassium were leached early as they are not bound to the C-S-H thus come in solution immediately. The high levels of calcium leached out from the cement account for the biocompatibility of MTA. Biocompatibility testing of cement leachables showed that the elution made up of a high concentration of CH produced during the hydration reaction induced cell proliferation. Cell growth was poor when seeded in direct contact with the test cements (Camilleri *et al.* 2005b). The MTA had a higher susceptibility to leaching. Both pastes were made to water to powder ratio of 0.5; however in the MTA this included the bismuth oxide. High water to cement ratios increases the susceptibility of the cement to leaching (Taylor 1997). The levels of bismuth and silica leached out of MTA increased with time. This relationship was verified by the SEM where a direct relationship between the silica and bismuth was shown in the atomic ratio plots. The bismuth does not act as filler in MTA but actively takes part in the hydration reaction. The XRD analysis showed a reduction in bismuth levels in the hydrated paste showing that bismuth was being used up in the hydration reaction. The bismuth replaced the silica in the C-S-H (verified by the straight line in the atomic ratio plot) then it is lost through leaching. This is again in accordance to a previous publication which shows that the bismuth actively took part in the hydration mechanism (Camilleri 2007). Bismuth oxide is soluble in acidic media (Lide 1998) thus, an acidic environment would likely increase the leaching of bismuth from the material. It has been demonstrated that bismuth oxide does not encourage cell growth and proliferation (Camilleri *et al.* 2004). However, addition of bismuth oxide to the Portland cement did not interfere with the biocompatibility of the material. Presumably the high concentration of calcium ions released from the material make up for the lack of cell proliferation on bismuth oxide.

Conclusions

Mineral trioxide aggregate and Portland cement are primarily composed of tricalcium and dicalcium silicate which on hydration produce C-S-H and CH. Tricalcium aluminate levels in MTA were found to be

lower than those of Portland cement leading to reduced production of ettringite and monosulphate on hydration. The hydration mechanism of MTA is different to that of Portland cement; in MTA the bismuth oxide is bound to the C-S-H and is leached out from the cement with time as the C-S-H decomposes. MTA produces a high proportion of calcium ions from CH a by-product of hydration and also by decomposition of C-S-H. The release of calcium ions reduces with time.

Acknowledgements

The University of Malta Research Grant Committee for funding. Heritage Malta for access to equipment and Mr Lawrence Spiteri for his assistance.

References

Adenot F, Buil M (1992) Modelling of corrosion of the cement paste by deionized water. *Cement and Concrete Research* **22**, 489–96.

Asgary S, Parirokh M, Eghbal MJ, Brink F (2004) A comparative study of white mineral trioxide aggregate and white Portland cements using X-ray microanalysis. *Australian Endodontic Journal* **30**, 89–92.

Camilleri J (2007) Hydration mechanisms of mineral trioxide aggregate. *International Endodontic Journal* **40**, 462–70.

Camilleri J, Montesin FE, Papaioannou S, McDonald F, Pitt Ford TR (2004) Biocompatibility of two commercial forms of mineral trioxide aggregate. *International Endodontic Journal* **37**, 699–704.

Camilleri J, Montesin FE, Brady K, Sweeney R, Curtis RV, Pitt Ford TR (2005a) The constitution of mineral trioxide aggregate. *Dental Materials* **21**, 297–303.

Camilleri J, Montesin FE, Di Silvio L, Pitt Ford TR (2005b) The chemical constitution and biocompatibility of accelerated Portland cement for endodontic use. *International Endodontic Journal* **38**, 834–42.

Dammaschke T, Gerth HU, Zuchner H, Schafer E (2005) Chemical and physical surface and bulk material characterization of white ProRoot MTA and two Portland cements. *Dental Materials* **21**, 731–8.

Duarte MA, De Oliveira Demarchi AC, Yamashita JC, Kuga MC, De Campos Fraga S (2005) Arsenic release provided by MTA and Portland cement. *Oral Surgery, Oral Medicine, Oral Pathology, Oral Radiology and Endodontics* **99**, 648–50.

Estrela C, Bammann LL, Estrela CR, Silva RS, Pecora JD (2000) Antimicrobial and chemical study of MTA, Portland cement, calcium hydroxide paste, Sealapex and Dycal. *Brazilian Dental Journal* **11**, 3–9.

Funteas UR, Wallace JA, Fochtman EW (2003) A comparative analysis of Mineral Trioxide Aggregate and Portland cement. *Australian Dental Journal* **29**, 43–4.

Gabrisova A, Havlika J, Sahu S (1991) Stability of calcium sulphoaluminate hydrates in water solutions with various pH values. *Cement and Concrete Research* **21**, 1023–7.

Gilfrich JV, Cev Novan I, Jenkins R *et al.* (1998) *Advances in X-ray analysis. Vol 39. Proceedings of the 44th Annual Conference on Applications of X-ray Analysis*. Colorado: University of Denver.

Lide DR (1998) *CRC Handbook of Chemistry and Physics*, 79th edn. Abingdon, UK: CRC Press, Taylor & Francis, pp. 1–10.

Mauras Y, Allain P (1979) Determination of barium in water and biological fluids by emission spectrometry with indirectively-coupled plasma. *Analityca Chimica Acta* **110**, 271–7.

Montaser A (1998) *Inductively Coupled Plasma Mass Spectrometry*. New York: Ed. Wiley VCH.

Oppenheimer JA, Eaton AD, Leong LYC (1984) *Multielemental analytical techniques for hazardous waste analysis: The state of art*. Las Vegas NV: US Environmental Protection Agency, Office of Research and Development, Environmental Monitoring Systems Laboratory. EPA600484028.

Rietveld HM (1969) A profile refinement method for nuclear and magnetic structure. *Journal of Applied Crystallography* **2**, 65–71.

Scrivener KL, Fullmann T, Gallucci E, Walenta G, Bermejo E (2004) Quantitative study of Portland cement hydration by X-ray diffraction/Rietveld analysis and independent methods. *Cement and Concrete Research* **34**, 1541–7.

Taylor HFW (1997) *Cement Chemistry*. London: Thomas Telford.

Torabinejad M, White DJ (1995) *Tooth filling material and use. US Patent Number 5,769,638*.

Torabinejad M, Hong CU, McDonald F, Pitt Ford TR (1995) Physical and chemical properties of a new root-end filling material. *Journal of Endodontics* **21**, 349–53.